Lumped-parameter-based thermal analysis for virtual prototyping of power electronics systems

W. Wang, X. Yuan

Department of Electrical and Electronic Engineering, The University of Bristol, United Kingdom, BS8 1UB,
wenbo.wang@bristol.ac.uk, xibo.yuan@bristol.ac.uk

Keywords: Virtual prototyping, lumped-parameter model, thermal analysis, power electronics system, steady state.

Abstract

Virtual prototyping of power electronics systems can enable rapid and iterative design process, and can satisfy the need for higher power density. Thermal modelling is a key part in the multi-physics virtual prototyping. In this paper, the T-type steady-state lumped-parameter model (LPM) for a naturally cooled heat sink with a power device on top is established. Empirical equations for the convection heat-transfer coefficient calculation are provided, which prove to be much faster compared with computational fluid dynamics (CFD) with acceptable error. The sensitivity of the predicted temperature to the mesh size of the heat sink for the LPM method is analysed, providing a way to find the most efficient mesh size. Lastly, the LPM is compared to the finite difference method (FDM) in steady state and shows competitive advantages in terms of speed and accuracy.

1 Introduction

Power electronics systems are very complex, including electrical, magnetic, thermal and mechanical domains and their coupling effect. The electrical and magnetic aspects have been the main research focus for a long time. Nevertheless, due to the demanding for higher power density, the thermal analysis and management of power electronics systems is becoming more and more important.

Most of the power electronics system design processes still depend on the empirical methods for the geometry and layout design, such as the heat sink selection, fan selection, and position arrangement of the components in the system. Multi-domain modelling and design tools based on virtual prototyping approaches [1-4] are needed to accurately determine the physical location and geometry of components for a high-density system. The virtual prototyping approach can enable quick evaluation of a large number of design possibilities on a computer. A key requirement for virtual prototyping is to generate a fast thermal analysis model which can be easily integrated with other models in different domains.

A lot of papers have been published on the thermal analysis model of power electronics systems. The research subject can be categorized into three levels: device/module level, board level and system level. The device/module level problems [5-8] establish thermal models for the substrate and the physical layers in the power electronic module, aiming to locate and calculate the temperature of the hotspot of the module. On the board level [9, 10], the power module is modelled as a unit, and the thermal performance of the power modules and other components on the heat sink or board is analysed. The system level [1, 11] includes all the components in a whole converter system. In this paper, the board level problem is analysed, as shown in Fig.1, which includes a natural cooled heatsink and a heat source representing a power electronics device, e.g. IGBT.

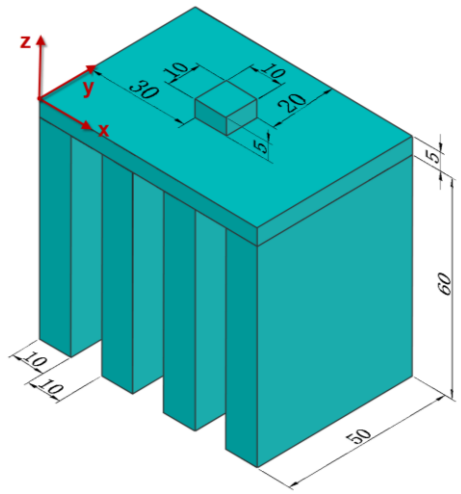

Fig.1 Dimension of the heat sink and power device

The methods that have been used in thermal analysis of power electronics are: computational fluid dynamics (CFD), finite element method (FEM), compact thermal model or empirical lumped-element model [5, 12], finite difference method (FDM) with model order reduction (MOR) [3], and lumped-parameter model (LPM) or physical lumped-element model [10]. In the methods above, CFD software can simulate the conduction and convection heat transfer together, which provides the most accurate and detailed temperature distribution of the power electronic system. But it is also the most demanding in terms of computer resources and computational time. The other methods can only simulate the conduction heat transfer, with the convection heat-transfer coefficient need to be calculated from empirical equations. As a numerical method, the speed and computation source usage of FEM are its disadvantages compared with the other three methods. The compact thermal model or empirical lumped-element model [5, 12] is quite simple and fast to solve, but the extraction process to get the model is very computationally

expensive. Lumped-parameter model (LPM) is widely used in thermal analysis of electrical machines [13], however it has not been paid much attention in the power electronics field. The scholars from University of Parma [12] used two resistor network of LPM for thermal analysis of power electronic devices and power device assemblies. However, as concluded in paper [14], the T-type network compared to the two resistor network can get more accurate average temperature. Therefore, in this paper, T-type LPM is used. In addition, heat sink is modelled as a flat plate in [10]. As the finned heat sink is also commonly used, in section 2, the detailed LPM for finned heat sink is established. And in section 3, the sensitivity of the temperature accuracy to the mesh size of the heat sink is analysed. In [3], Evans introduced MOR method to solve the FDM equations with quite fast speed. But MOR does not accelerate the calculation speed in steady state condition. In section 4, the LPM is compared with the FDM for the steady state thermal analysis.

2 Lumped-parameter thermal model

Analogous to electric circuits, the LPM for thermal analysis, as a kind of analytical method, represents the heat transfer path by connecting a series of thermal resistances. And the heat source is represented by current source in the model. There are three thermal phenomenon in the power electronics system: radiation, conduction and convection. Correspondingly, there are three types of thermal resistances: radiation, conduction and convection thermal resistances, among which radiation is always ignored compared to conduction and convection.

2.1 Conduction thermal resistances

The conduction exists in solid materials. Based on the steady state heat diffusion equation (1) and the Fourier's law (2) [15], the LPM T-network for one dimensional heat transfer is shown in Fig.2 and the thermal resistances are shown in Equation (3-4) [14]. It can be seen that the conduction thermal resistances can be calculated easily from the geometry dimension and the material thermal properties.

$$\frac{\partial^2 T}{\partial x^2} = -\frac{q_x}{k} \tag{1}$$

$$q_x = -k_x A_x \frac{\partial T}{\partial x} \tag{2}$$

$$R_{x1} = R_{x2} = \frac{l_x}{2k_x A_x} \tag{3}$$

$$R_{x3} = -\frac{l_x}{6k_x A_x} \tag{4}$$

Where, q_x is the heat-transfer rate (W), $\partial T/\partial x$ is the temperature gradient in the direction of heat flow (^oC / m), k_x is the thermal conductivity of the material (W/(m·^oC)), A_x is the cross area in the direction of heat flow (m^2), and l_x is the length of the solid material in the direction of heat flow (m).

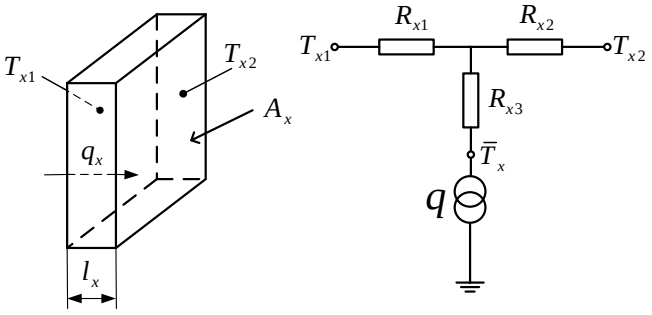

Fig.2 LPM for one dimensional heat transfer

Based on the one dimensional LPM, the LPM for three dimensional heat transfer in cuboid geometry can be derived, as shown in Fig.3. In power electronic systems, the heat sink and the power device are both of regular geometry, which can be divided into several cuboids. Then the LPM for each cuboid is connected together to form the whole model for the system.

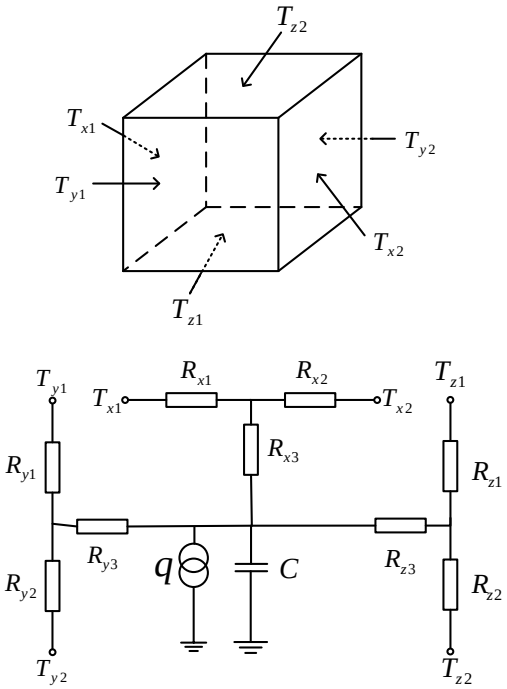

Fig.3 LPM for three dimensional heat transfer

2.2 Convection thermal resistances

The convection heat transfer occurs on the surface between the solid components and air or liquid, depending on the cooling method used. Water-cooling, forced-air cooling and natural air cooling are the most common cooling methods in power electronics systems. The convection plays an important part in the cooling of power electronic system, thus the accuracy of convection thermal resistance estimation is important for the thermal analysis.

In LPM, based on the Newton's law of cooling (5), the convection thermal resistance is shown as Equation (6).

$$q = hA(T_w - T_\infty) \tag{5}$$

$$R = \frac{\Delta T}{q} = \frac{1}{hA} \tag{6}$$

Where, T_w is the solid surface temperature (^oC), T_∞ is the fluid temperature (^oC), h is the convection heat-transfer coefficient (W/(m$^2\cdot{}^oC$) and A is the surface area (m^2).

The convection heat-transfer coefficient is the key parameter for the convection thermal resistance determination. There are three types of methods for convection heat-transfer coefficient estimation: analytical solution [15], CFD [16] and empirical equations [15]. Analytical solutions can only be available for very limited conditions. CFD, as a numerical method, is quite accurate, but it is much demanding in terms of computer resources and computational time. By contrast, empirical equations which are the results of experimental data have a broader application and are easy and fast to get the convection heat-transfer coefficient. Therefore, normally empirical equations are used in LPM.

For the problem discussed in this paper, the natural convection heat-transfer coefficient of the heat sink is the key parameter, the empirical equations for which in [17] are used, as shown in Equation (7-9).

$$Ra = \frac{\rho^2 g \beta c_p z^4 (T_w - T_\infty)}{\mu k L} \tag{7}$$

$$Nu = \frac{Ra}{24}\left(1 - e^{-35/Ra}\right)^{3/4} \tag{8}$$

$$h = k \cdot Nu / z \tag{9}$$

Where, Ra is the Rayleigh number, Nu is the Nusselt number, ρ is the air density (kg/m^3), β is the coefficient of cubical expansion ($1/K$), c_p is the air specific heat capacity ($kJ/(kg\cdot{}^oC)$), μ is the air dynamic viscosity ($kg/(s\cdot m)$), k is the air thermal conductivity ($W/(m\cdot{}^oC)$), g is the gravitational attraction force (m/s^2), z is the heat sink fin spacing (m), L is the heat sink fin length (m).

2.3 Comparison of LPM and CFD

In this section, the problem is analysed using LPM and CFD to verify the LPM. The heat sink is divided/meshed into cuboids each of which is represented by the T-network as shown in Fig.3. The LPM for this problem is shown in Fig.4, in which the grey blocks represent the T-network for heat sink cuboid divisions, the red block represents the T-network for IGBT, the voltage source represents the temperature of the ambient air, and the resistances represent the convection thermal resistances between heat sink and the ambient air. The natural convection heat-transfer coefficient is calculated from the empirical equations (7-9). MATLAB is applied to generate the LPM netlist in NGSpice. Fig.4 shows the schematic diagram of the LPM in which the heat sink is divided into 44 elements. To get a more detailed temperature distribution, the heat sink is divided into 6592 elements, the temperature distribution of which is shown in Fig.5.

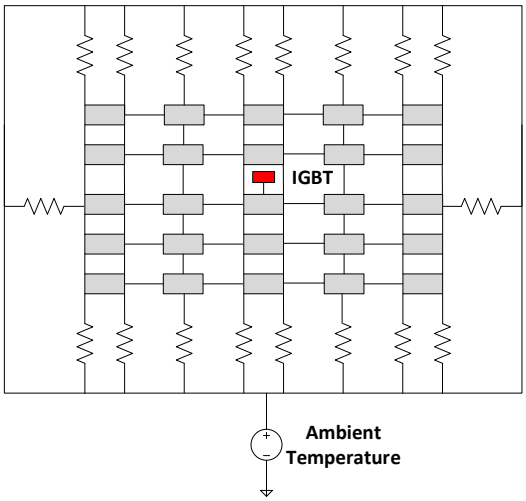

Fig.4 LPM for heat sink and IGBT

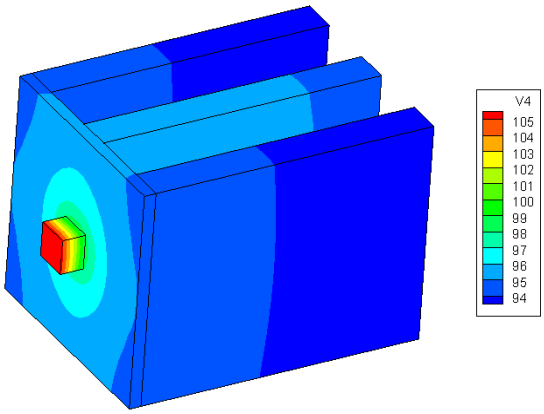

Fig.5 Temperature distribution by using LPM

To test the accuracy of LPM method, the problem is also analysed by CFD in ANSYS. The temperature distribution of the heat sink and IGBT is shown in Fig.6. Table 1 gives the analysis results, including the convection heat-transfer coefficient of the heat sink calculated from the empirical equations and from the CFD, the temperature of IGBT calculated from LPM and from CFD, as well as the time used by LPM and CFD.

From the results in Table 1, two conclusions can be derived. Firstly, it can be seen that results difference between these two lumped-parameter models of different detail level is less than 1%. The reason is that the equations of conduction thermal resistances for regular geometries, such as cuboids and cylinders, are analytical solutions of the energy partial differential equation, which is weekly impacted by the mesh size, quite different from the numerical methods. Therefore, quite accurate results can be got from simple model, saving computational time and computer resources. Secondly, compared to CFD, the error of convection heat-transfer

coefficient calculated from empirical equations is acceptable, and the speed is much faster than CFD simulation.

	h_heatsink (W/(m·K))	T_IGBT (ºC)	Time
LPM_Fig4	9.60	106.88	1 second
LPM_Fig5	9.65	106.40	1 hour
CFD	8.6	108	20 hours

Table 1 Results of LPM and CFD

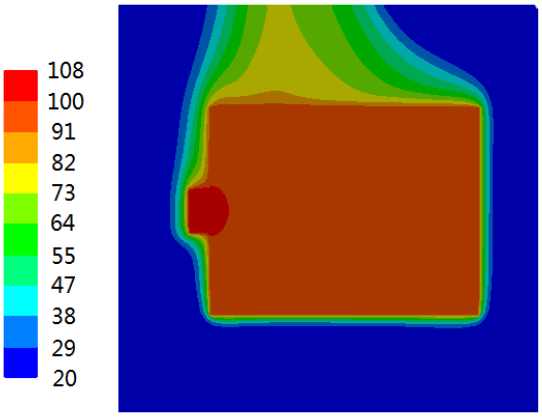

Fig.6 Temperature distribution by using CFD

3 Sensitivity of LPM

As stated in section 2, the results difference between two lumped-parameter models of different detail level is less than 1%, however, the time consumed by the larger model is much longer. So in this section, the sensitivity of LPM is researched, which means to search how the mesh size of each element determines the temperature accuracy and to find the most efficient mesh size for heat sink LPM thermal analysis.

The dimensions of the heat sink and IGBT discussed in this paper are shown in Fig.1. And the results for the sensitivity analysis are shown in Table 2. In this analysis, the ANSYS and LPM use the same natural convection heat-transfer coefficient, and the ANSYS result is the reference for LPM sensitivity analysis. In Table 2, the mesh sizes in x, y and z direction are changed successively to discuss how the mesh size in each direction influences the results accuracy.

Firstly, in x direction, as the fin length is 10 millimetres, the maximum mesh size of the heat sink fin should be 10mm. As the fin gap is also 10mm, to represent the geometry of the heat sink clearly and to give an accurate position of the IGBT which locates at 30mm in the x direction, the maximum mesh size of the heat sink base is also 10mm. The maximum mesh size of the IGBT is 10mm, which is the total length of the IGBT in x direction. The "LMP-X2" row in Table 2 shows the results error to be 1.16% when the heat sink fin, heat sink base and IGBT mesh size in x direction is 10mm. The "LMP-X1" row in Table 2 increases the heat sink base mesh size in x direction to 30/10/30, which can give an accurate description of the IGBT position but not enough for the heat sink geometry description, getting much larger error of 4%. The "LMP-X3" row decreases the mesh size but only get a small decrease of error. So it can be seen that in x direction, the mesh size 10mm which represents geometry clearly and gives accurate position description is the most efficient.

When in y direction, the mesh size in x direction is set to be 10. And the "LPM-Y2" row shows the results error to be 1.43%, when the mesh size in y direction is 20/10/20, which describes the IGBT position accurately. In comparison, the "LPM-Y1" row increases the mesh size in y direction to be 50 and gets the results error of -2.06%, a minus error which is not safe for temperature estimation. And the "LPM-Y3" row decreases the mesh size in y direction to be 0.5 which is 40 times smaller than the "LPM-Y2" row, but only get a small change of error with ten times of time consumed. Therefore, in y direction, the mesh size which is the largest mesh size to describe the position of IGBT is the most efficient. In z direction, the same conclusion can be achieved. And the mesh sizes in x, y and z direction in "LPM-Z1" row are the most efficient with a quite small error.

Based on the analysis above, the most efficient mesh size for LPM is the largest one which can give clear geometry description, and the results error can be quite small.

4 Comparison of LPM and FDM

Finite difference method (FDM) is a kind of numerical methods for solving the partial differential equation (PDE) [18]. The PDE for 3D transient state thermal analysis is shown as Equation (10). The principle of FDM for solving steady state PDE can be summarised as the following steps. Firstly, the research subject is meshed into cuboid elements. Then the second derivatives in PDE are replaced by the finite difference approximations according to Taylor's series expansion, as shown in Equation (11). In this way, the PDEs of the study area are discretised into a large system of algebraic equations on nodes. For transient state problems the time space is discretised and the steady state equations are solved at each time point.

MOR is introduced to speed up the transient state FDM solving process [3]. The feature of MOR techniques is their simplification of the large system of equations into a system with fewer equations and fewer unknown variables. A smaller equation system is generated using the MOR technique for the steady state equations firstly, then the smaller equation system is solved at each time points to get the transient solutions. Therefore, MOR can speed up the transient FDM dramatically. However, as the computational cost of generating the reduced order model, the MOR does not maintain its advantage in steady state. In this paper, the results of LPM are compared with the FDM without MOR for the steady state thermal analysis.

$$c\rho\frac{\partial T}{\partial t}-k\left(\frac{\partial^2 T}{\partial x^2}+\frac{\partial^2 T}{\partial y^2}+\frac{\partial^2 T}{\partial z^2}\right)=q \qquad (10)$$

	Heat sink fin mesh size (mm)			Heat sink base mesh size (mm)			IGBT mesh size (mm)			Mesh number	Results		Time (s)
	x	y	z	x	y	z	x	y	z		IGBT (ºC)	Error (%)	
LPM-X1	10	10	60	30 /10 /30	10	5	10	10	5	36	106.22	4.13	1
LPM-X2	10	10	60	10	10	5	10	10	5	56	103.20	1.16	1
LPM-X3	5	10	60	5	10	5	5	10	5	112	103.04	1.01	1
LPM-Y1	10	50	60	10	50	5	10	10	5	12	99.91	-2.06	1
LPM-Y2	10	20 /10 /20	60	10	20 /10 /20	5	10	10	5	34	103.47	1.43	1
LPM-Y3	10	0.5	60	10	0.5	5	10	0.5	5	1120	103.16	1.13	10
LPM-Z1	10	20 /10 /20	60	10	20 /10 /20	5	10	10	5	34	103.47	1.43	1
LPM-Z2	5	10	1	5	10	1	5	10	1	2760	102.42	0.40	80
Ansys											102.01		

Table 2 Sensitivity analysis results

$$\frac{\partial^2 T}{\partial x^2} \approx \frac{1}{h^2}\left(T_{i-1,j,k} - 2T_{i,j,k} + T_{i+1,j,k}\right) \tag{11}$$

Where, c is the specific heat capacity of the material ($J/(kg{\cdot}^oC)$), h is the mesh size (m).

The large system of equations can be transferred into matrix equation format, the coefficient matrix of which is very sparse, with each row having maximum 7 non-zeros for 3D problems. Two solvers are used to solve the large matrix equation. One is the successive over relaxation (SOR) method, a kind of iterative solution method. The other one is the KLU method [19], which is a solver for sparse matrix. The IGBT temperature and the time consumed by using FDM with SOR and KLU solvers and by LPM method are shown in Table 3, where the ANSYS result is the reference. The temperature distribution of the FDM is shown in Fig.7.

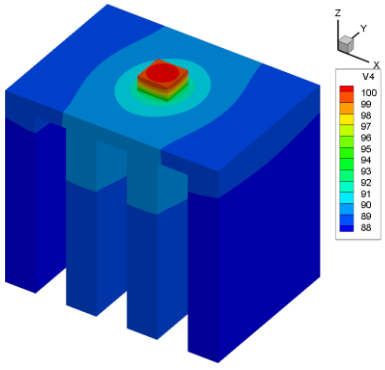

Fig.7 Temperature distribution by using FDM

	Mesh number	T_IGBT	Error (%)	Time (s)
FDM with KLU	1104	80.16	-21	1
	8832	94.25	-7	1
	70656	100.64	-1.3	15
FDM with SOR	1104	85.75	-16	7
	8832	97.18	-4.7	100
	70656	102.12	0.11	1600
LPM	34	103.47	1.43	1
ANSYS		102.01		

Table 3 Results of LPM and FDM

It can be seen that KLU solver is much faster than the SOR solver. When the mesh number is about 70K, the time consumed by KLU solver is 15 seconds, while for SOR it is 1600s. However, the SOR solver gets more accurate results at the same mesh size. When the mesh number is 70K, the error of KLU is -1.3% while for SOR the error is only 0.11%. In addition, as a type of numerical method, the FDM results are influenced largely by the mesh size. For FDM with KLU solver, the error changes from -21% with 1K meshes to -1.3% with 70K meshes. By contrast, the LPM can get quite accurate results with small mesh numbers at much faster

speed. The error for LPM is 1.43% with only 34 meshes in less than 1 second time.

5 Conclusion

This work has established the LPM for the steady state thermal analysis of the basic power electronics system element (heat sink and power device). And sensitivity analysis of the temperature accuracy to the mesh size of the LPM shows that the LPM can estimate the temperature very accurately with small mesh numbers in short time. Although the research subject in this paper is quite simple, the other components in power electronics system, such as the conductors, capacitors and transformers, can also be simplified to regular geometry, such as cuboids and cylinders, which can also be modelled in the same way. Similarly, this method can also be applied for the module level analysis. Therefore, LPM for different detail levels of power electronics system can be established depending on the specific problem and target. In the future work, the LPM will be used for the transient state thermal analysis of power electronics system, the result accuracy and speed of which will be compared to the FDM with MOR method.

Acknowledgements

The authors would like to thank the UK EPSRC National Centre for Power Electronics under Grant EP/K035096/1 for supporting the related research.

References

[1] J. Biela, J.W. Kolar, A. Stupar, U. Drofenik, and a. A. Muesing, "Towards Virtual Prototyping and Comprehensive Multi-Objective Optimisation in Power Electronics," *Power Electronics*, vol. 6, 2010.

[2] P. L. Evans, A. Castellazzi, and C. M. Johnson, "A Multi-Disciplinary Virtual Prototyping Design Tool for Power Electronics," in *Integrated Power Systems (CIPS), 2014 8th International Conference on*, 2014, pp. 1-7.

[3] P. L. Evans, A. Castellazzi, and C. M. Johnson, "Design Tools for Rapid, Multi-Domain Virtual Prototyping of Power Electronic Systems," *Power Electronics, IEEE Transactions on*, vol. 31, pp. 2443-2455, Mar. 2016.

[4] P. Solomalala, J. Saiz, A. Lafosse, M. Mermet-Guyennet, A. Castellazzi, X. Chauffleur, *et al.*, "Multi-domain simulation platform for virtual prototyping of integrated power systems," in *Power Electronics and Applications, 2007 European Conference on*, 2007, pp. 1-10.

[5] P. L. Evans, A. Castellazzi, and C. M. Johnson, "Automated Fast Extraction of Compact Thermal Models for Power Electronic Modules," *IEEE Transactions on Power Electronics*, vol. 28, pp. 4791-4802, Oct. 2013.

[6] P. L. Evans, A. Castellazzi, S. Bozhko, and C. M. Johnson, "Automatic design optimisation for power electronics modules based on rapid dynamic thermal analysis," in *Power Electronics and Applications (EPE), 2013 15th European Conference on*, 2013, pp. 1-10.

[7] F. Bertoluzza, G. Sozzi, N. Delmonte, and R. Menozzi, "Hybrid Large-Signal/Lumped-Element Electro-Thermal Modeling of GaN-HEMTs," *Microwave Theory and Techniques, IEEE Transactions on*, vol. 57, pp. 3163-3170, Dec. 2009.

[8] M. Bernardoni, N. Delmonte, G. Sozzi, and R. Menozzi, "Large-signal GaN HEMT electro-thermal model with 3D dynamic description of self-heating," in *Solid-State Device Research Conference (ESSDERC), 2011 Proceedings of the European*, 2011, pp. 171-174.

[9] P. Cova and M. Bernardoni, "A MATLAB based approach for electro-thermal design of power converters," in *Integrated Power Electronics Systems (CIPS), 2010 6th International Conference on*, 2010, pp. 1-5.

[10] M. Bernardoni, N. Delmonte, P. Cova, and R. Menozzi, "Self-consistent compact electrical and thermal modeling of power devices including package and heat-sink," in *Power Electronics Electrical Drives Automation and Motion (SPEEDAM), 2010 International Symposium on*, 2010, pp. 556-561.

[11] P. Cova, N. Delmonte, F. Giuliani, M. Citterio, S. Latorre, M. Lazzaroni, *et al.*, "Thermal optimization of water heat sink for power converters with tight thermal constraints," *Microelectronics Reliability*, vol. 53, pp. 1760-1765, Jul. 2013.

[12] P. C. Roberto Menozzi, Nicola Delmonte, Francesco Giuliani, Giovanna Sozzi, "Thermal and electro-thermal modeling of components and systems: a review of the research at the university of parma," *FACTA UNIVERSITATIS Series: Electronics and Energetics*, vol.28, pp. 325-344, Sept. 2015.

[13] P. H. Mellor, D. Roberts, and D. R. Turner, "Lumped parameter thermal model for electrical machines of TEFC design," *Electric Power Applications, IEE Proceedings B*, vol. 138, pp. 205-218, 1991.

[14] R. Wrobel and P. H. Mellor, "A General Cuboidal Element for Three-Dimensional Thermal Modelling," *Magnetics, IEEE Transactions on*, vol. 46, pp. 3197-3200, Aug. 2010.

[15] J.P.Holman, *Heat transfer*. New York: McGraw-Hill, 2010.

[16] F. M. White, *Fluid mechanics.* New York: McGraw-Hill, 2010.

[17] A. D.Kraus, *Design and analysis of heat sinks*. New York: Wiley-Interscience, 1995.

[18] G. D. Smith, *Numerical solution of partial differential equations : finite difference methods*. Oxford Clarendon Press 1985.

[19] T. A. Davis and E. P. Natarajan, "Algorithm 907: KLU, A Direct Sparse Solver for Circuit Simulation Problems," *ACM Trans. Math. Softw.*, vol. 37, pp. 1-17, Sept. 2010.